3-1995

A Spectroscopic and Photometric Study of 12 BM Camelopardalis

Douglas S. Hall
Vanderbilt University

Francis C. Fekel
Vanderbilt University

Gregory W. Henry
Tennessee State University

Joel A. Eaton
Tennessee State University

William S. Barksdale

See next page for additional authors

THE ASTRONOMICAL JOURNAL VOLUME 109, NUMBER 3 MARCH 1995

A SPECTROSCOPIC AND PHOTOMETRIC STUDY OF 12 BM CAMELOPARDALIS

DOUGLAS S. HALL AND FRANCIS C. FEKEL

Dyer Observatory, Vanderbilt University, Nashville, Tennessee 37235
Electronic mail: hallxxds@ctrvax.vanderbilt,edu, fekelxfc@ctrvax.vanderbilt.edu

GREGORY W. HENRY AND JOEL A. EATON

Center of Excellence in Information Systems, Tennessee State University, Nashville, Tennessee 37203
Electronic mail: henry@coe.tnstate.edu, eaton@coe.tnstate.edu

WILLIAM S. BARKSDALE

633 Balmoral Road, Winter Park, Florida 32789

VIRGILIJUS DADONAS

Vilnius Astronomical Observatory, Ciurlionio 29, 2009 Vilnius, Lithuania
Electronic mail: virgilijus.dadonas@ff.vu.lt

ZEKI EKER

Astronomy Department, King Saud University, Riyad 11451, Saudi Arabia
Electronic mail: f40a010@saksu00.bitnet

PEEP KALV

Tallinn Observatory, Tahetorni 2, EE-0016 Tallinn, Estonia

CARLSON R. CHAMBLISS

Physical Science Department, Kutztown University, Kutztown, Pennsylvania 19530

ROBERT E. FRIED

Braeside Observatory, P.O. Box 906, Flagstaff, Arizona 86002
Electronic mail: braeside@naucse.cse.nau.edu

GEORGE L. FORTIER

63 Devon Road, Baie d'Urfe, Quebec H9X 2W7, Canada

HOWARD J. LANDIS

50 Price Road West, Locust Grove, Georgia 30248

HOWARD P. LOUTH

2199 Hathaway Road, Sedro Woolley, Washington 98284

HARRY D. POWELL

Department of Physics, East Tennessee State University, Johnson City, Tennessee 37614
Electronic mail: r29harry@etsu.bitnet

THOMAS G. MCFAUL

Shenandoah Observatory, 870 Pequot Avenue, Southport, Connecticut 06490

RICHARD MILES

Manley Observatory, Fernbank Farm, Sugar Lane, Manley, Cheshire WA6 9DZ, England

PAUL NIELSEN

Dublin Observatory, 1817 Shipley Road, Wilmington, Delaware 19803

THOMAS R. RENNER

Scuppernong Observatory, 4512 Deerpark Drive, Dousman, Wisconsin 53118

STEPHEN P. ROBB

211 West Greentree Drive, Tempe, Arizona 85284

 0004-6256/95/109(3)/1277/12/$0.90

DOUGLAS M. SLAUSON
Summit Observatory, 73 Summit Avenue, Route 1, Box 383, Swisher, Iowa 52338

HAROLD J. STELZER[1]
1223 Ashland Avenue, River Forest, Illinois 60305

RICK WASSON
Sunset Hills Observatory, 15870 Del Prado Drive, Hacienda Heights, California 91745

JAMES E. WOOD
Faun Lane Observatory, 11732 Faun Lane, Garden Grove, California 92641

Received 1994 October 26; revised 1994 November 28

ABSTRACT

Radial velocities from 1916.95 to 1991.95 and photometry from 1979.25 to 1992.40, both published and new in this paper, are presented and analyzed. A new solution of the radial velocity curve reveals a new period of $80^{d}.90$ and an eccentricity of $e=0.05\pm0.02$, both very different from the $80^{d}.17$ and 0.35 found by Abt *et al.* [ApJ, 157, 717 (1969)]. An alternative solution with $e=0$ is given because we cannot decide firmly whether or not the small eccentricity is real. We find $V \sin i=11.3\pm0.3$ km/s from Maidanak and 10 km/s from Kitt Peak. Fourier analysis of the V-band photometry shows the ellipticity effect with minima of unequal depth, $0^{m}.048$ and $0^{m}.026$. The orbital ephemeris for conjunction (K giant behind) is JD(hel.) 2,448,111.1 ($\pm0^{d}.4$)+$80^{d}.898$ ($\pm0^{d}.004$) E, consistent with both the radial velocities and the photometry. With the ellipticity effect removed, the light curve shows residual variability which we fit with a two-spot model. During the 13 years covered by photometry there were nine different starspots, the largest one producing a light loss of $0^{m}.19$. Rotation periods for the nine spots ranged from $78^{d}.6\pm0^{d}.5$ to $83^{d}.7\pm0^{d}.4$, from which we concluded that the K giant does rotate synchronously but with a differential rotation coefficient of $k=0.06\pm0.01$. Lifetimes for the nine spots ranged from 1.1 to >4.2 yr and were consistent with the empirical spot lifetime laws of Hall & Henry [IAPPP Comm. No. 55, 51 (1994)]. Use of the mass function, the orbital period, the $V \sin i$, the two different ellipticity effect amplitudes, and various logical constraints led to ranges of possible masses, radii, and inclinations. The most believable solution was around $i=90°$, $R_1=24\ R_\odot$, $\mathcal{M}_1=1.1\ \mathcal{M}_\odot$, and $\mathcal{M}_2=0.6\ \mathcal{M}_\odot$. The Rossby number for the K giant is 0.48, small enough compared to the critical value of 0.65 to explain why, though rotating "slowly," it does have large spots.

1. INTRODUCTION

The bright ($V=6.1$) star 12 BM Cam=HR 1623=HD 32357 is an SB1 with an early K-type giant in an 80-day orbit. The first and only published spectroscopic orbit is that of Abt *et al.* (1969), which showed the orbit to be eccentric ($e=0.35\pm0.02$). Photometric variability was discovered by Eaton *et al.* (1980), who attributed the variability to rotational modulation of dark starspot regions on the K giant. The only spectral classification seems to be the K0 III of Bidelman (1964). Additional observational characteristics are given in the catalogue of Strassmeier *et al.* (1993), where it appears as No. 48.

Hall & Busby (1989) showed that the photometric behavior was puzzling in several ways and did not succeed in solving all of those puzzles. There were multiple periodicities in the 1979–1988 photometry they analyzed. One was $79^{d}.93\pm0^{d}.05$, which they identified with the orbital period and attributed to the ellipticity effect. There was more power at P(orb.) than at P(orb.)/2, they concluded, because the two minima differed markedly in depth.

One puzzle was that the $80^{d}.174469$ orbital period found by Abt *et al.* (1969) was inconsistent with the $79^{d}.93\pm0^{d}.05$ value, but they argued that the longer value could be in error, due to aliasing problems.

They noted that the large $e=0.35$ eccentricity should be causing the star-to-star distance to vary more than a factor of 2, $(1+0.35)/(1-0.35)=2.1$, during each orbital cycle, thereby modulating the amplitude of the ellipticity effect, and the value of ω near 90° should have resulted in equal maxima along with unequal minima, as observed. A second puzzle, however, was that the light variation predicted by such a periastron–apastron effect did not represent the actual shape of the light variation observed.

Two other periodicities, $82^{d}.5$ in the data up through 1984.5 and $81^{d}.0$ in the data after that, they attributed to rotational modulation of large dark starspot regions on the K giant at those epochs and used as measures of the K star's rotation period. The pseudosynchronous rotation period corresponding to an eccentricity of $e=0.35\pm0.02$ would be $45^{d}.2\pm2^{d}.5$ (Hall 1986), so the K star was far from pseudo-

[1]Deceased, October 7, 1994.

TABLE 1. Radial velocities.

JD(hel.) 2400000+	Phase	V_R (km/s)	O-C (km/s)	wt.	Wavelength (Å)	Source
21209.830	0.477	-6.6	-0.3	0.1	blue	1
21291.677	0.485	-6.8	-2.0	0.1	blue	1
21529.028	0.420	-9.2	3.7	0.1	blue	1
39430.856	0.695	13.3	-3.2	0.1	blue	2
.856	0.695	13.3	-3.2	0.0	Ca II H&K	2
39460.824	0.070	-12.6	-0.8	0.1	blue	2
.824	0.070	-9.8	2.0	0.0	Ca II H&K	2
39461.862	0.083	-15.6	-2.3	0.1	blue	2
.862	0.083	-12.0	1.3	0.0	Ca II H&K	2
39515.739	0.749	17.8	0.3	0.1	blue	2
.739	0.749	13.4	-4.1	0.0	Ca II H&K	2
39517.775	0.774	20.0	2.8	0.1	blue	2
.775	0.774	16.5	-0.7	0.0	Ca II H&K	2
39775.913	0.965	4.2	2.8	0.1	blue	2
.913	0.965	-1.5	-2.9	0.0	Ca II H&K	2
39776.857	0.977	1.8	1.8	0.1	blue	2
.857	0.977	-3.3	-3.2	0.0	Ca II H&K	2
39871.935	0.152	-19.1	0.7	0.1	blue	2
.935	0.152	-21.7	-1.9	0.0	Ca II H&K	2
39903.694	0.545	3.4	0.8	0.1	blue	2
.694	0.545	0.2	-2.4	0.0	Ca II H&K	2
39908.648	0.606	10.0	0.4	0.1	blue	2
.648	0.606	11.9	2.3	0.0	Ca II H&K	2
45266.929	0.838	13.2	-1.2	0.1	blue	3
45746.599	0.767	17.55	0.3	0.1	6560	4
.599	0.767	17.61	0.3	0.0	Hα	4
45760.583	0.940	8.21	3.7	0.1	6560	4
.583	0.940	7.60	3.1	0.0	Hα	4
45769.602	0.052	-7.08	2.4	0.1	6560	4
.602	0.052	-7.90	1.6	0.0	Hα	4
45783.622	0.225	-23.63	-0.3	0.1	6560	4
.622	0.225	-23.85	-0.5	0.0	Hα	4
47624.684	0.982	-0.3	0.3	1.0	6430	5
47627.704	0.019	-6.0	-0.4	1.0	6430	5
47932.130	0.782	16.81	-0.2	1.0	3900-6900	6
47937.185	0.844	13.82	-0.2	1.0	3900-6900	6
47940.243	0.882	11.43	0.6	1.0	3900-6900	6
47943.261	0.920	6.64	-0.3	1.0	3900-6900	6
47947.163	0.968	-0.04	-1.1	1.0	3900-6900	6
47950.193	0.005	-4.15	-0.5	1.0	3900-6900	6
48162.987	0.636	12.5	0.1	1.0	6430	5
48167.972	0.697	15.6	-0.7	1.0	6430	5
48346.603	0.905	8.0	-0.5	1.0	6430	5
48506.009	0.876	12.0	0.6	1.0	6430	5
48507.020	0.888	10.3	0.1	1.0	6700	5
48508.993	0.912	8.1	0.4	1.0	6430	5
48576.997	0.753	17.9	0.4	1.0	6560	5
48604.826	0.097	-14.5	0.3	1.0	6430	5
48605.945	0.111	-16.1	0.1	1.0	6430	5

1 = Adams and Joy (1923)
2 = Abt, Dukes, Weaver (1969)
3 = Eitter (1991)
4 = Eker, this paper
5 = Fekel, this paper
6 = Dadonas, this paper

synchronism. Given asynchronous rotation in an eccentric orbit, a continuous range of rotation rates is possible, both faster and slower than the pseudosynchronous rate, and the value $P(\text{rot.})=P(\text{orb.})$ is of no special significance. A third puzzle was the finding that, fortuitously, $P(\text{rot.})\approx P(\text{orb.})$ afterall.

In this paper we bring additional radial velocity measures and photometry to bear on the problem. Some of this has been published elsewhere in the meantime, i.e., after the paper of Hall & Busby (1989), but most of it is presented for the first time here. The full set of radial velocity measures now extends from 1916.95 through 1991.95, and the available photometry from 1979.25 through 1992.40.

2. NEW SPECTROSCOPIC ORBIT AND CORRECT ORBITAL PERIOD

Table 1 lists all of the radial velocity measures known for BM Cam. The first 24, previously published, are from Adams & Joy (1923), Abt *et al.* (1969), and Eitter (1991). The last of these, a single observation originally appearing in Beavers & Eitter (1986), has been remeasured (Eitter 1991) and this new value is the one given in our table. The last 25 have been obtained by us and are given here for the first time.

Eker made observations on four nights in 1984 at the Pine Bluff Observatory of the University of Wisconsin with the 0.91 m reflector and an intensified Reticon detector attached to the echelle spectrograph. The spectra are of echelle order 37, which contained Hα and a number of metal lines, and have a resolution of 0.16 Å. Velocities for the Hα and metal lines were computed separately. Additional information about the processing and analysis of these spectra is given in Eker (1986).

From 1989 to 1991 Fekel obtained 11 observations at Kitt Peak National Observatory with the coudé feed telescope, coudé spectrograph, and a Texas Instruments CCD. The spectra had a wavelength range of 80 Å, a resolution of 0.2 Å, and nearly all were centered at 6430 Å. One observation was obtained of the lithium region at 6707 Å and one was obtained at Hα. Most of the spectra have signal-to-noise ratios of 100:1 or better. The radial velocities were determined relative to several International Astronomical Union radial velocity standard stars (Pearce 1957). From the work of Scarfe *et al.* (1990), we assumed velocities of 3.2 km/s for β Gem, 4.4 km/s for β Vir, and 27.9 km/s for 10 Tau. Details of the velocity reduction procedure have been given by Fekel *et al.* (1978). The value $V \sin i = 10$ km/s given in Strassmeier *et al.* (1993) had been estimated from some of these spectra.

On Mt. Maidanak in Pamir, Uzbekistan, Dadonas obtained six observations in 1990 February with the 1 m Lithuanian reflector and a photoelectric radial velocity scanner similar to CORAVEL (Tokovinin 1987). Each radial velocity is determined by cross correlation between the stellar spectrum and a mask of about 200 metal lines in the 3900–6900 Å region. The projected rotational velocity derived from the mean width of the cross-correlation profile was $V \sin i = 11.3 \pm 0.3$ km/s.

It was immediately apparent that the orbital period found by Abt *et al.* (1969), $80^{d}.174469 \pm 0^{d}.000003$, did not fit the new velocities and must not be correct. A periodogram based on successive sinusoidal fits over a range of assumed periods, seen in Fig. 1, shows that the correct period is $80^{d}.9$, although the $80^{d}.17$ value does appear with much weaker power as an alias. The total variance is reduced to 1.5% with $80^{d}.9$ but only to 40% with $80^{d}.17$.

With the correct orbital period we determined a new spectroscopic orbit. The velocities of Fekel and Dadonas were given unit weight, the Hα velocities of Eker and the Ca II H and K emission line velocities of Abt *et al.* (1969) were given zero weight, and all other velocities were given a weight of 0.1. Because of the small number of velocities in most data sets and their relatively poor phase coverage, no attempt was made to shift the velocity zero point of any set. Since no large systematic velocity differences are evident, it appears that the various zero points are in reasonable accord. The resulting solution, with the correct period, resulted in an eccentricity of 0.05 ± 0.02, considerably smaller than the

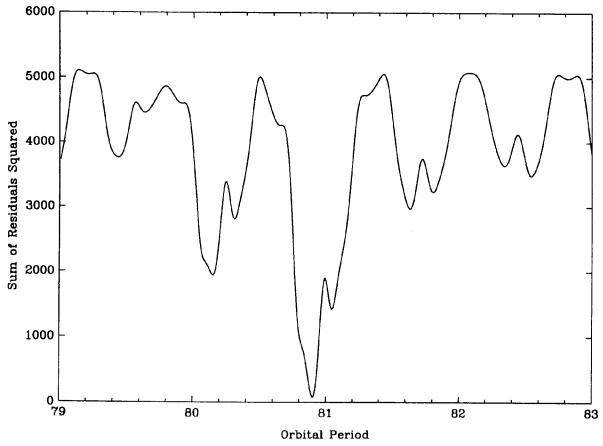

FIG. 1. A periodogram of the available radial velocities, based on successive sinusoidal fits over a range of assumed periods. This shows that the correct period is $80^d.9$, although the $80^d.17$ value of Abt *et al.*(1969) does appear with much weaker power as an alias.

$e=0.35$ value in the Abt *et al.* (1969) solution. In an attempt to determine if this small eccentricity is real, we applied the precepts of Lucy & Sweeney (1971), which were based on significance at the 5% level, equivalent to $e=2.45\ \sigma$. By this criterion, $e=0.05\pm0.02$ is on the edge between accepting and rejecting. To decide definitively between the circular and the slightly eccentric, additional observations will be needed, especially in the large gap between phase 0.12 and 0.62 with no unit-weight observations. Because the reality of the small eccentricity is not certain, we provide an alternate solution forced to be circular. The phases (from conjunction, K giant behind) and residuals given in Table 1 pertain to this circular orbit.

Table 2 lists the orbital elements for both the circular and the eccentric solutions. Comparison of the two center-of-mass velocities as well as the two semiamplitudes indicates differences slightly greater than the sum of their uncertainties. These modest differences may result from the previously mentioned gap in the phase coverage. The orbital period was determined explicitly in both cases and the resulting values, along with the times of conjunction (K giant behind),

TABLE 2. Orbital elements.

	circular	eccentric
T(peri)	---	2448109.8 ± 4.3
K_1 (km/sec)	20.5 ± 0.3	19.2 ± 0.6
γ (km/sec)	-3.0 ± 0.3	-2.0 ± 0.6
e	---	0.05 ± 0.02
ω (degrees)	---	86 ± 20
f(M) ($M_\odot$)	0.072 ± 0.003	0.060 ± 0.005
$a_1 \sin i$ (Gm)	22.8 ± 0.3	21.4 ± 0.7

TABLE 3. Orbital ephemeris.

Period	Conjunction	Data source	Method
80.901 ±.003	2448111.5 ±.2	velocities weighted	circular orbit
80.895 ±.004	2448110.7 ±.2	velocities weighted	eccentric orbit
80.872 ±.052	2448109.24 ±.64	photometry ΔV	cos 2θ
80.951 ±.054	2448110.69 ±.61	photometry ΔV	cos 2θ, cos θ
80.835 ±.048	2448108.12 ±.59	photometry $\Delta_L V$	cos 2θ
80.912 ±.053	2448109.81 ±.58	photometry $\Delta_L V$	cos 2θ, cos θ
80.916 ±.012	2448110.12 ±.17	photometry $\Delta_S V$	cos 2θ
80.910 ±.009	2448109.97 ±.14	photometry $\Delta_S V$	cos 2θ, cos θ

are given in Table 3. Figure 2 is a plot of all 49 radial velocities, compared with the circular orbit shown as the solid curve. The Hα and Ca II H and K velocities, though given zero weight in the solution, appear to be consistent with the other velocities.

For computing orbital phases in the rest of this paper, we adopt the ephemeris

$$\text{JD(hel.)}=2{,}448{,}111.1+80^d.898E, \quad (1)$$
$$\pm.4 \quad \pm.004$$

the mean of the circular and the eccentric solution, where the initial epoch is conjunction with the K giant behind.

3. PHOTOMETRIC DATA

All photometry discussed in this paper was done differentially with respect to a comparison star, in almost every case HR 1688=HD 33618, corrected for differential atmospheric extinction, and transformed differentially to the appropriate

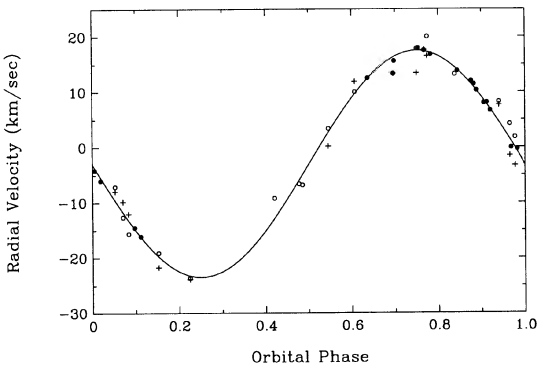

FIG. 2. A plot of all 49 radial velocities given in Table 1 compared with the circular orbit given in Table 2 and shown here as the solid curve. Filled circles, open circles, and crosses indicate weights of 1.0, 0.1, and 0.0 used in the solution. The Hα and H&K velocities, though given zero weight in the solution, appear to be consistent with the other velocities.

bandpass of the *UBV* system. We restrict our study to the *V* bandpass, the only bandpass used by all of the observers. In almost every case a single value of ΔV is actually a mean of about three differential magnitudes resulting from a *C-V-C-V-C-V-C* sequence of observation, where *C* is the comparison star and *V* is the variable.

The early 1979 and early 1980 photometry discussed by Eaton *et al.* (1980) was not published in that paper but was available in our files. Archive file No. 121 described by Breger (1985) contained late 1980 photometry by J. A. Eaton at Kitt Peak National Observatory and Archive File No. 147 described by Breger (1987) contained 1984 photometry also by Eaton at Kitt Peak. In the 1983 photometry by Fernandes (1983) 11 Cam=HR 1622 was used as a comparison star, but we compensated by adding $-0^{m}.995$ to the ΔV magnitudes in his table. The extensive photometry obtained with the 10-in. automatic telescope between late 1983 and late 1987 was taken from Boyd *et al.* (1990). The problem caused by the yellow filter dropping out in the summer of 1985, which they called Problem D, did not affect BM Cam, which is not observable during the summer.

The observatories contributing new, i.e., not yet published, photometry are listed in Table 4. Descriptions of many of these observatories are given by Hall & Genet (1988, Table 8-1): Braeside, Dublin, E.T.S.U., Louth, Mouldsworth, Nielsen, Scuppernong, Shenandoah, Stelzer, and Sunset Hills. The Vanderbilt–Tennessee State 16-in. automatic telescope has been described most recently by Hall & Henry (1993) and by Henry & Hall (1994). This new photometry has not yet been sent to the I.A.U. Commission 27 Archive for Unpublished Observations of Variable Stars or other such archive but is available in digital form from this paper's first author upon request.

TABLE 4. New photometry.

Observatory	Location	Aperture inch	Aperture cm	Observers
Barksdale	Florida	14	35	Barksdale
Braeside	Arizona	16	40	Fried
Dublin	Delaware	4	10	Nielsen
Dyer	Tennessee	24	60	Henry
E.T.S.U.	Tennessee	8	20	Powell
Fortier	Quebec	12.5	32	Fortier
Kitt Peak	Arizona	16	40	Henry
Kutztown	Pennsylvania	15	38	Chambliss
Landis	Georgia	8	20	Landis
Louth	Washington	11	28	Louth
McDonald	Texas	30	75	Henry
"	"	36	90	Henry
Mouldsworth	England	11	28	Miles
Mt. Hopkins	Arizona	16	40	Hall,Henry
Scuppernong	Wisconsin	10	25	Renner
Shenandoah	New York	14	35	McFaul
Stelzer	Illinois	14	35	Stelzer
Summit	Iowa	8	20	Slauson
Sunset Hills	California	8	20	Wasson
Tallinn	Uzbekistan	--	48	Kalv
Vilnius	Uzbekistan	--	48	Dadonas
Robb	Arizona	10	25	Robb
Faun Lane	California	10	25	Wood

4. LONG-TERM LIGHT VARIATION

Figure 3 is a plot of all of the ΔV magnitudes, which cover the 13-year span between 1979 March and 1992 May. Variability on a time scale of some years is apparent. A periodogram shows power at a period of 2298 ± 34 days$=6.3 \pm 0.1$ years. A sinusoidal fit at this period yields a full amplitude of $0^{m}.068 \pm 0^{m}.004$. The significance of this variation, if any, will be discussed later. The overall amplitude of the light curve in any given year, $0^{m}.15$ to $0^{m}.20$, results from the combined effect of ellipticity and starspots, as discussed in the next two sections.

5. REMOVING THE ELLIPTICITY EFFECT

The first analysis performed on the ΔV magnitudes was a period search in the vicinity of the orbital period, to see if the ellipticity effect was present. We did this by making successive cos 2θ fits. The resulting best period is listed in Table 3, along with a time of minimum light, which would correspond to a time of conjunction. We applied the period search again to the ΔV magnitudes after the long-term light variation (found in Sec. 4) had been removed, by subtracting a sinusoid with a 6.3-year period and a $0^{m}.07$ full amplitude. We call these the $\Delta_L V$ magnitudes. The resulting best period and corresponding time of minimum light are listed in Table 3 as well. Both the periods and the implied times of conjunction, as determined from the two data sets, are in agreement within their respective errors.

Because Hall & Busby (1989) had found unequally deep minima when they detected the ellipticity effect, we repeated the period search with a truncated Fourier series containing terms in both cos 2θ and cos θ. We did this to both the ΔV and the $\Delta_L V$ magnitudes. The resulting best periods and times of conjunction are listed in Table 3, where we see they are consistent with each other and with the values found by the cos 2θ fits.

Note that the photometry has yielded values for both the period *and* the time of conjunction which are very close to the corresponding values in Eq. (1) which came from the radial velocity curve solution. For the period, there is agreement within the respective uncertainties. For the times of

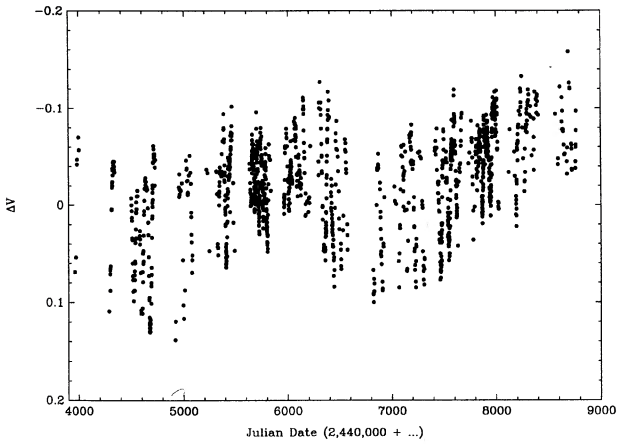

FIG. 3. A plot of all ΔV magnitudes, which cover the 13-year span between 1979 March and 1992 May. Variability on a time scale of some years is apparent. A periodogram shows power at 2298±34 days=6.3±0.1 years and a sinusoidal fit at this period yields a full amplitude of $0^m.068 \pm 0^m.004$. The amplitude of the light curve in any given year, $0^m.15$ to $0^m.20$, results from the combined effect of ellipticity and starspots.

conjunction the agreement is not quite as good, with the photometric times being systematically earlier by a little more than 1 standard deviation. Given such agreement, we do not hesitate to conclude that our $\cos 2\theta$, $\cos \theta$ fit does represent the ellipticity effect. Because the orbital eccentricity is so small, it is doubtful that any sort of periastron–apastron effect can be producing the unequal minima in the ellipticity effect. We now know, however, that unequal minima can be understood most reasonably as a consequence of enhanced limb-darkening and gravity-darkening effects on the pointed end of the K giant, the "pointed and effect" discussed by Hall (1990a).

We removed the ellipticity effect from the entire set of ΔV magnitudes by subtracting a light curve of the form

$$\Delta V = -0^m.025 + 0^m.018 \cos 2\theta + 0^m.011 \cos \theta, \qquad (2)$$

where the θ is computed with the adopted orbital ephemeris in Eq. (1). The coefficients in Eq. (2) are those from the $\cos 2\theta$, $\cos \theta$ fit to the ΔV magnitudes. In that curve the two minima have depths of $0^m.048$ and $0^m.026$, as measured from the two maxima, which are equal in height. The light curve thus cleaned of the ellipticity effect will be referred to as the $\Delta_E V$ magnitudes.

6. REPRESENTING THE STARSPOT VARIABILITY

Experience with other spotted variables has shown (Hall & Busby 1990; Hall & Henry 1994) that starspots have lifetimes no longer than a few years and sometimes less than a year and, moreover, that the amplitude of the light variation produced by rotational modulation changes throughout a given spot's lifetime. Therefore it was necessary to avoid analyzing a data set which spanned too long a time interval. On the other hand, it is obvious that a data set should span an appreciable fraction of the rotation period in order to be useful. The 33 data sets listed in Table 5 are the ones decided upon, after some trial and error, for analysis. The first column is the data set's identifying number, the second column is its median epoch, the third column is the number of $\Delta_E V$ magnitudes it contains, and the last column is the number of days it spans.

TABLE 5. Data sets.

Set	Median epoch	n	Δt
1	1979.75	31	376
2	1980.88	57	127
3	1981.20	62	98
4	1982.08	33	160
5	1982.69	2	10
6	1982.91	23	121
7	1983.20	67	73
8	1983.37	18	37
9	1983.89	94	63
10	1984.10	87	77
11	1984.29	48	57
12	1984.83	57	94
13	1985.10	39	86
14	1985.31	22	69
15	1985.75	56	94
16	1985.99	36	78
17	1986.25	23	98
18	1987.21	32	107
19	1987.71	12	70
20	1987.93	18	72
21	1988.12	32	59
22	1988.33	15	59
23	1988.79	53	78
24	1989.04	75	90
25	1989.29	45	81
26	1989.71	38	105
27	1989.95	85	67
28	1990.16	103	78
29	1990.32	23	32
30	1990.78	31	119
31	1991.06	24	68
32	1991.29	16	83
33	1992.12	32	199

Figure 4 is a plot of the $\Delta_E V$ magnitudes versus Julian date for the years 1980–81 through 1991–92. Some of them include more than one of the adopted data sets. Others consist entirely of one data set.

We applied the two-spot light curve fitting procedure first devised by Hall *et al.* (1990) to study V478 Lyr. This procedure has since been applied productively to V1817 Cyg (Hall *et al.* 1990), V1149 Ori (Hall *et al.* 1991a), λ And (Hall *et al.* 1991b), HU Vir (Hall & Henry 1992a), and HD 191262 and HD 191011 (Hall & Henry 1992b). Resulting parameters of the best fits, those resulting in the minimum value of the sum of the squares of the residuals, are listed in Table 6. The first column is the data set number. The second column is the Julian date of light minimum, a time when the spot faces

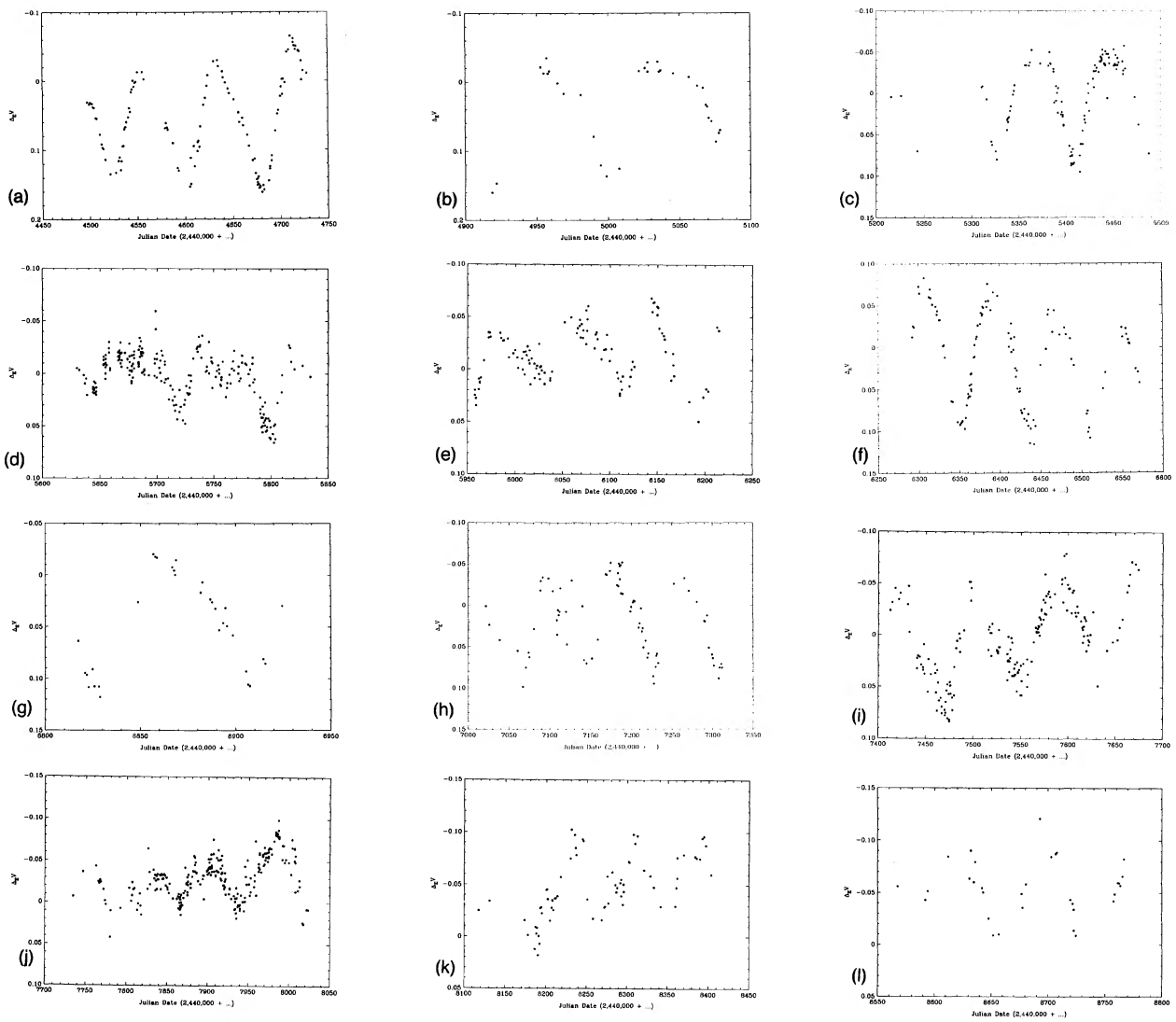

FIG. 4. Plots of the $\Delta_E V$ magnitudes vs Julian date for the years 1980–81 through 1991–92. Some of these 12 panels include more than one of the adopted data sets listed in Table 5; others consist entirely of one data set. These light curves, from which the ellipticity effect *has been removed*, were fit with the two-spot model of Hall *et al.* (1990).

Earth, taken in the middle of the data set's time span. The third column is the light loss produced by that spot. The fourth and fifth columns are the same, for the second spot. The sixth column is the $\Delta_E V$ value at maximum light, when neither of the two spots is visible. The seventh column is the slope of any gradual brightening or dimming which occurred throughout the data set, in units of magnitude per day, negative for brightening, positive for dimming. The last column is the rms deviation from the best fit.

Although the fitting procedure of Hall *et al.* (1990) included the rotation periods of the two spots as two of the seven fitting parameters, we fixed the rotation period at 81 days in a few cases where the phase coverage was not sufficient for an explicit determination. In some cases (data sets 5, 6, 7, 8, 9, and 29) only one spot was required to represent the light curve. In one case, data set 5, a minimum was well defined but the coverage of the maximum was lacking, so we adopted a value of $\Delta_E V$(max.) by interpolation between data sets 4 and 6.

7. THE MIGRATION CURVE, SPOT PERIODS, AND SPOT LIFETIMES

For each of the values of JD(min.) in Table 6 we computed phase with the adopted orbital ephemeris in Eq. (1). These are plotted in Fig. 5, with fractional phase, θ(min.), on the vertical axis and whole phase, E, on the horizontal axis. Note that θ(min.) is equivalent to longitude on the K star, with θ=0.0 being the longitude facing the companion star, θ=0.5 being the longitude away from the companion star, and θ=0.25 and θ=0.75 being the longitudes orthogonal to the major axis of the binary. E, of course, is equivalent to time. In such a plot, called a migration curve, a spot with a constant rotation period would have its points follow a

TABLE 6. Spot parameters.

	First Spot		Second Spot				
Set	JD(min.) 2440000+	ampl. (mag.)	JD(min.) 2440000+	ampl. (mag.)	$\Delta_E V$(max.) (mag.)	slope (mag./day)	rms (mag.)
1	4289.0	0.165	4326.0	0.042	-0.038	0.00000	0.009
2	4602.8	0.133	4488.0	0.055	+0.004	0.00000	0.010
3	4683.0	0.188	4658.0	0.079	-0.035	-0.00030	0.011
4	4917.4	0.161	4976.7	0.035	-0.023	0.00000	0.011
5	------	-----	5220.3	0.042	[-0.034]	0.00000	-----
6	5328.1	0.110	------	-----	-0.039	0.00000	0.006
7	5408.1	0.112	------	-----	-0.037	0.00000	0.013
8	5847.3	0.111	------	-----	-0.037	0.00000	0.008
9	5637.7	0.029	------	-----	-0.014	0.00000	0.009
10	5718.7	0.056	5759.6	0.034	-0.028	0.00000	0.012
11	5798.5	0.082	5844.3	0.054	-0.031	0.00000	0.010
12	5952.4	0.060	6004.6	0.036	-0.041	-0.00026	0.007
13	6096.5	0.027	6117.8	0.066	-0.047	-0.00030	0.009
14	6169.8	0.059	6195.2	0.095	-0.058	0.00000	0.008
15	6339.0	0.074	6355.9	0.122	-0.058	+0.00025	0.009
16	6414.9	0.044	6437.8	0.141	-0.045	+0.00025	0.013
17	6497.4	0.052	6516.3	0.104	-0.022	+0.00025	0.008
18	6898.3	0.060	6914.9	0.082	-0.012	0.00000	0.008
19	7035.8	0.072	7067.4	0.108	-0.028	0.00000	0.007
20	7114.7	0.070	7150.8	0.125	-0.054	0.00000	0.018
21	7201.2	0.046	7227.2	0.125	-0.049	0.00000	0.012
22	7284.4	0.026	7308.0	0.106	-0.029	0.00000	0.008
23	7445.8	0.064	7471.5	0.105	-0.039	0.00000	0.014
24	7526.5	0.047	7553.1	0.077	-0.035	0.00000	0.011
25	7622.2	0.056	7645.8	0.076	-0.057	-0.00020	0.013
26	7784.2	0.051	7810.3	0.027	-0.033	0.00000	0.012
27	7863.0	0.041	7893.7	0.015	-0.045	-0.00030	0.010
28	7934.4	0.058	7959.0	0.026	-0.062	-0.00035	0.012
29	8025.7	0.082	------	-----	-0.058	0.00000	0.014
30	8180.3	0.096	8206.9	0.056	-0.088	0.00000	0.010
31	8262.4	0.100	8291.6	0.062	-0.107	0.00000	0.008
32	8334.4	0.030	8350.8	0.045	-0.084	0.00000	0.010
33	8648.9	0.064	8669.0	0.056	-0.093	0.00000	0.012

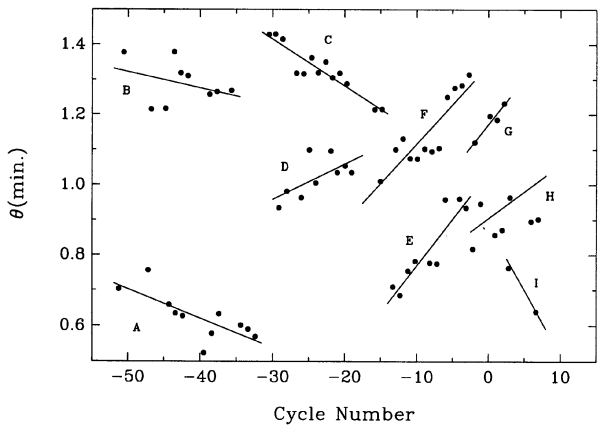

FIG. 5. The JD(min.) values in Table 6 plotted as a migration curve, with the adopted orbital ephemeris in Eq. (1) used to compute phases. Fractional phase, θ(min.), is the vertical axis and whole phase, E, is the horizontal axis; θ(min.) is equivalent to longitude on the K star, with θ=0.0 being the longitude facing the companion star. A spot with a constant rotation period would have its points follow a straight-line segment, sloping up if P(rot.) >P(orb.) and down if P(rot.)<P(orb.). The length of each line segment would represent the lifetime of that spot. There are more points here than there are values of JD(min.) in Table 6 because some of the data sets spanned more than one complete rotation cycle.

straight-line segment, sloping up if P(rot.)>P(orb.) and down if P(rot.) <P(orb.). The length of each line segment would represent the lifetime of the corresponding spot. There are more points in Fig. 5 than there are values of JD(min.) in Table 6 because some of the data sets spanned more than one complete rotation cycle. The additional points are obtained simply by adding or subtracting one value of P(rot).

The corresponding values of the spot amplitudes, from columns 3 and 5 of Table 6, are plotted in Fig. 6, again with E as the horizontal axis. Experience with other spotted variables leads us to anticipate that a given spot's amplitude will evolve smoothly with time, generally rising to a maximum and then falling. Apparently this comes about as a spot comes into existence, grows in size, and then decays by a mechanism not yet known, possible mechanisms being decreasing size, diminishing temperature contrast with the surrounding photosphere, or disruption by differential rotation (Hall & Busby 1990; Hall & Henry 1994).

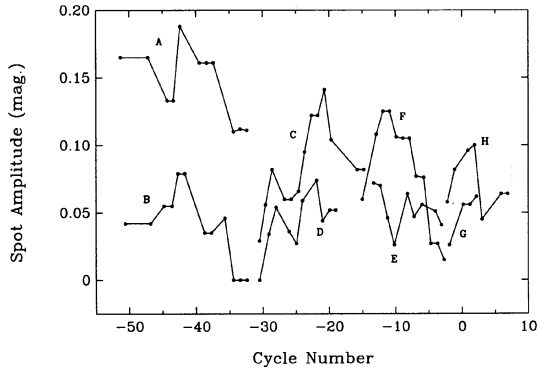

FIG. 6. The corresponding values of the spot amplitudes from Table 6, again with E as the horizontal axis. Note that most of these spot amplitudes evolve smoothly with time, rising to a maximum and then falling, presumably as a spot comes into existence, grows in size, and then decays.

TABLE 7. Spot periods, maximum amplitudes, and lifetimes.

Spot	m	Period (days)	rms (days)	max.ampl. (mag.)	L(obsv.) (years)	L(calc.) (years)
A	11	80.23 ± 0.19	3.3	0.188	>4.18	6.03
B	9	80.56 ± 0.38	4.4	0.079	>3.46	4.34
C	13	79.85 ± 0.12	2.0	0.141	3.54	6.84
D	9	81.73 ± 0.38	3.4	0.074	2.39	3.85
E	9	83.11 ± 0.40	3.8	0.072	2.43	3.62
F	12	82.79 ± 0.34	4.0	0.125	2.98	7.28
G	4	82.97 ± 0.52	1.3	0.062	1.10	2.69
H	7	81.24 ± 0.52	4.0	0.100	>2.34	7.43
I	2	78.63 ± 0.50	---	>0.070	>1.22	>3.41

By applying the criteria of constancy of slope and continuity of phase in Fig. 5, and smoothness of evolution in Fig. 6, we identified nine spots that have been present on the surface of the K giant during the 13 years of our photometry. These are designated A through I.

For the eight spots having more than two values of JD (min) available, those values were fit by linear least squares to determine each spot's rotation period. These are tabulated in Table 7, where the second column gives the number of values of JD(min.) included in each fit, the third column is the rotation period itself, and the fourth column is the rms deviation from the fit. The average rms deviation is about $\pm 3^d.3$ or $\pm 0^p.04$. The period for the last spot, I, was based on only two values of JD(min.) so its uncertainty comes from the uncertainty of those two values. These 9 periods are represented as the straight-line segments in Fig. 5.

The lifetime of each spot, taken as the difference between the beginning date of the first data set in which it first appeared and the end of the last data set in which it was last seen, is entered in the next-to-last column of Table 7. Understandably, lifetime estimates will be lower limits for those spots already present in data set 1 and those still present in data set 33.

8. THE ELLIPTICITY EFFECT

Although we made a preliminary determination of the light variation due to the ellipticity effect, that was done with the starspot variability still present in the light curve, with its greater amplitude. Now we are in a position to remove the spot variability, as represented by the parameters in Table 6, from the original ΔV magnitudes and thereby reveal the ellipticity effect with superior definition. The light curve thus cleaned of the spot variability we call the $\Delta_s V$ magnitudes. Period searches with both cos 2θ and cos 2θ, cos θ fits resulted in the periods and times of conjunction which appear as the last two entries in Table 3. They, too, are generally consistent with the values derived from the radial velocities, and their uncertainties are less than those from fits to the ΔV or $\Delta_L V$ magnitudes.

Figure 7 shows the ellipticity effect, as a plot of the $\Delta_s V$

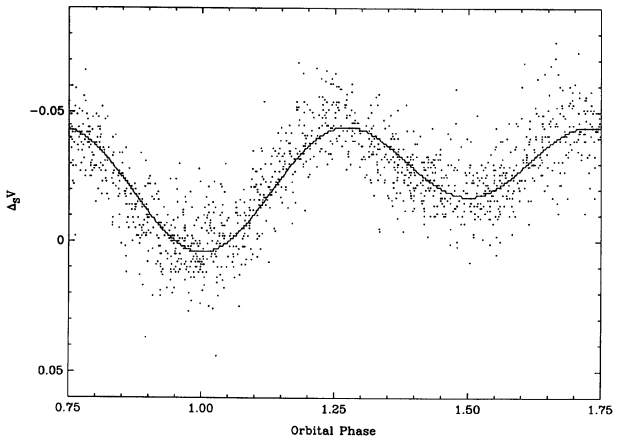

FIG. 7. The ellipticity effect, shown as a plot of the $\Delta_3 V$ magnitudes vs orbital phase computed with the ephemeris in Eq. (1). The solid curve represents the fit with a $\cos 2\theta$, $\cos\theta$ curve having coefficients of $0^m.0184 \pm 0^m.0004$ and $0^m.0105 \pm 0^m.0004$, respectively, which compares favorably with the corresponding preliminary values in Eq. (2). The two minima have depths of $0^m.049$ and $0^m.027$, as measured from the two maxima, which are equal in height.

TABLE 8. Possible masses and radii.

i (deg.)	F	R_1 ($R_\odot$)	M_1 ($M_\odot$)	M_2 ($M_\odot$)	D (mag.)	Condition
V sin i = 11.3 km/s						
19	1.00	55	3.6	5.6	0.000	F < 1
29	0.83	37	1.9	2.2	0.000	ΔB > 2 mag.
31	0.79	31	1.7	1.9	0.000	M_2/M_1 < 1.1
53	0.62	23	0.9	0.7	0.000	M_1 > 0.9 $M_\odot$
90	0.54	18	0.6	0.4	0.015	i < 90°
V sin i = 15 km/s						
20	1.00	69	6.6	6.8	0.000	F < 1
32	0.79	45	3.2	2.5	0.000	ΔB > 2 mag.
90	0.56	24	1.1	0.6	0.016	i < 90°

magnitudes versus orbital phase computed with the ephemeris in Eq. (1). The coefficients of the $\cos 2\theta$ and $\cos\theta$ terms are $0^m.0184 \pm 0^m.0004$ and $0^m.0105 \pm 0^m.0004$, respectively, which can be compared with the corresponding preliminary values which appeared in Eq. (2). With these coefficients the two minima have depths of $0^m.049$ and $0^m.027$, as measured from the two maxima, which are equal in height. The difference in the depths is $D = 0^m.022$, a quantity we will use later.

9. THE RADIUS AND MASS OF THE K GIANT

Although BM Cam is an SB1 and not known to be eclipsing, we can use the known $V \sin i$ and our determination of the amplitude of the ellipticity effect, following generally the procedure outlined by Hall (1990a), to place useful constraints on the masses of the two stars, the radius of the K giant, and the orbital inclination. Specifically, we take the mass function corresponding to the spectroscopic elements in Table 2, $f(\mathcal{M}) = 0.065\ \mathcal{M}_\odot$ (a mean of the $e=0$ and the $e=0.05$ solutions), $V \sin i = 15 \pm 3$ km/s from Huisong & Xuefu (1987) or 11.3 ± 0.3 from our paper, and the depth of the shallower of the two minima of the ellipticity effect, $0^m.027$.

Alternative solutions are given in Table 8 for both values of $V \sin i$. The column headings are orbital inclination i, Roche-lobe-filling fraction F, radius of the K giant R_1, mass of the K giant $\mathcal{M}_1$, mass of the unseen secondary $\mathcal{M}_2$, and difference D between the two minima of the ellipticity effect resulting from the pointed-end effect. Each of these solutions represents an upper or lower limit imposed by one of five possible constraints. First, $F<1$, meaning the K giant cannot overfill its Roche lobe. Second, $\Delta B > 2$ mag, meaning the secondary star must be at least 2 mag fainter than the primary in the blue spectral region so that it be unseen in the spectrum, which is the case. Third, $\mathcal{M}_2/\mathcal{M}_1 < 1.1$, so that the evolved K giant be the originally more massive star, after having lost no more than about 10% of its mass during the enhanced stellar wind stage (Tout & Hall 1991). Fourth, $\mathcal{M}_1 > 0.9\ \mathcal{M}_\odot$, so that the K giant can have evolved within the age of the galaxy. Fifth, $i<90°$.

The tightest limits are provided by the third and fourth constraints in the $V \sin i = 11.3$ km/s case, and by the second and third constraints in the 15 km/s case. In both cases, however, the extreme with the smallest radius is favored if one believes the K0 III classification of Bidelman (1964) was sufficiently precise to exclude K0 III-II or K0 II. Of those two favored solutions, the one based on 11.3 km/s is worrisome because it would predict $D = 0^m.000$, incompatible with the $D = 0^m.022 \pm 0^m.001$ seen in Fig. 7. The one based on 15 km/s, on the other hand, is much more nearly consistent. As an aside, we note that, even if the value $e=0.05$ in the eccentric solution is considered real, the periastron–apastron effect discussed by Hall & Busby (1989) could produce $D = 0^m.005 \pm 0^m.002$ but no more. Thus we are led to argue that the most believable solution is the $i=90°$, $F=0.56$, $R_1 = 24\ R_\odot$, $\mathcal{M}_1 = 1.1\ \mathcal{M}_\odot$, $\mathcal{M}_2 = 0.6\ \mathcal{M}_\odot$ solution based on $V \sin i = 15$ km/s. This solution would imply BM Cam is an eclipsing system, but eclipses of or by a (presumed main-sequence) star of $0.6\ \mathcal{M}_\odot$ would be less than $0^m.001$ deep and not detectable in our photometry, so that is not a concern. It is, however, a little worrisome that we are led to favor a solution based on the $V \sin i = 15 \pm 3$ km/s value, which has the greater uncertainty and is formally inconsistent with the 11.3 ± 0.3 km/s value. We can suggest that the dark regions present when the Dadonas spectra were taken might have distorted the line profile shapes in such a way as to diminish their effective widths.

10. DIFFERENTIAL ROTATION

A mean of the nine values in Table 7 is $81^d.23 \pm 0^d.14$, an estimate of the K giant's rotation period based on the motion of its spots. The full range of those nine values is $4^d.48$

$\pm 0^d.64$, i.e., $\Delta P/P = 5.5\% \pm 0.8\%$. Presuming that these differing rotation periods result from differential rotation as a function of latitude on the K giant, we can estimate the coefficient k as it appears in the equation

$$P(\phi)/P(\phi = 0°) = 1/(1 - k \sin^2 \phi) \quad (3)$$

commonly used to describe such differential rotation. Following the procedure of Hall & Henry (1994) to adjust for the fact that those nine spots probably do not sample the entire 90° latitude range, we get $k = 0.058 \pm 0.008$. The Sun, for comparison, has $k = 0.18$.

11. UNDERSTANDING THE STARSPOT LIFETIMES

Hall & Henry (1994) found that the lifetimes of starspots observed to date could be represented by a two-part law, the first being a function of the star's rotation period and differential rotation coefficient and the spot's angular diameter, the second being a function of the star's absolute radius and the spot's angular radius. A given spot's angular diameter can be determined from the amplitude of the light variation it produces. We have all of the quantities needed to see if the lifetimes of the nine spots listed in Table 7 are in accord with this two-part law. For the K giant's radius we use 24 $R_\odot$.

The calculated values are entered in the last column of Table 7. The four observed lifetimes that were lower limits are consistent with the theoretically expected values; those which were not just lower limits are systematically shorter but only by a factor of 2. Hall & Henry (1994) had found systematically good agreement between observed and calculated with an rms deviation of about 0.3 in the log, or a factor of 2. The two-part law is such that a spot's lifetime is supposed to be the lesser of the two times calculated with the two parts of the law, the first part applying generally to larger spots and the second part generally to smaller spots. In this case, spots B, D, E, G, H, and I proved to be "small" whereas A, C, and F proved to be "large."

12. CONCLUDING DISCUSSION

The 6.3-year periodicity found in the mean brightness probably is *not* manifestation of a long-period magnetic cycle such as discussed by Hall (1990b) but rather just a reflection of the fact that the starspot amplitudes generally rise to a maximum and fall and that the two spots generally present at any given epoch tend to emerge and die in concert. A periodogram of the quantity which is the sum of the amplitudes of the two spots present in each of the 33 data sets yields a period which is virtually identical (6.4 ± 0.3 yr vs 6.3 ± 0.1 yr), a full amplitude which is comparable ($0^m.12$ vs $0^m.07$), and a time of minimum brightness which is nearly in phase (1980.63 ± 0.15 vs 1981.25 ± 0.05). This interpretation is confirmed by the absence of any significant periodicity in the magnitude at maximum light, the quantity Δ_E(max.) of Table 6. The magnitude at maximum does, however, show a much slower secular trend, which might be a manifestation of a magnetic cycle several decades in length. The median magnetic cycle length found by Hall (1990b; Table 1) in a sample of 12 different types of convective stars was 30 years.

Because the large eccentricity originally suspected by Abt *et al.* (1969) has proven not to be real, the coincidence of P(rot.)$\approx P$(orb.) which puzzled Hall & Busby (1989) is no longer a puzzle. The K giant is simply rotating synchronously or, if the small eccentricity we find is real, pseudo-synchronously. If $e = 0$ and the rotation is synchronous, then the two quantities $81^d.23 \pm 0^d.14$ and $80^d.901 \pm 0^d.003$ should be nearly equal, which they are. If $e = 0.05 \pm 0.02$ and the rotation is pseudosynchronous, then the two quantities $81^d.23 \pm 0^d.14$ and $79^d.5 \pm 1^d.0$ should be nearly equal, which they are.

Hall & Henry (1990, Fig. 2) showed that orbital eccentricity in binaries containing an evolved late-type star can be understood very well by application of circularization time scale theory developed by Tassoul (1988). They demonstrated that, if the evolved star has expanded beyond some critical radius, which is a function of that star's mass and the binary's orbital period, then the orbit will have become circular. Conversely, all eccentric orbits are found in binaries whose evolved star is less than that critical radius. The K giant in BM Cam has a critical radius somewhere between 10 $R_\odot$ and 16 $R_\odot$ for a mass between 1.0 $\mathcal{M}_\odot$ and 3.0 $\mathcal{M}_\odot$, respectively. Because its radius today is considerably larger than this, between 24 $R_\odot$ and 45 $R_\odot$, respectively, we expect the orbit to have become well circularized. This consideration would suggest that the value $e = 0.05 \pm 0.02$ in Table 2 may be regarded as not significantly different from zero.

Heavy starspot coverage is now known to occur on stars which experience strong dynamo action due to rapid rotation, but is a rotation period of 81 days "rapid"? Strong dynamo action is specified more completely by Rossby number, Ro, defined as the ratio of the rotation period to the convective turnover time, and the critical value Ro = 0.65 is the threshold segregating the heavily spotted (strongly variable) stars from the unspotted or minimally spotted (nonvariable) stars (Hall 1991, 1994). The $80^d.9$ rotation period along with the convective turnover time of a K0 III star (Hall 1991, 1994) implies Ro = 0.48, small enough to account for the large starspots observed.

This work was supported in part by NASA Grants Nos. NAG 8-111 and NAG 8-1014 and by NSF Grant No. HRD-9104484.

REFERENCES

Abt, H. A., Dukes, R. J., & Weaver, W. B. 1969, ApJ, 157, 717
Adams, W. S., & Joy, A. H. 1923, ApJ, 57, 149
Beavers, W. I., & Eitter, J. J. 1986, ApJ, 62, 147
Bidelman, W. H. 1964, ApJ, 139, 405
Boyd, L. J., Genet, R. M., Hall, D. S., Busby, M. R., & Henry, G. W. 1990, IAPPP Comm. No. 42, 44
Breger, M. 1985, PASP, 97, 85
Breger, M. 1987, PASP, 100, 951

Eaton, J. A., Hall, D. S., Henry, G. W., Landis, H. J., McFaul, T. G., & Renner, T. R. 1980, IBVS No. 1902
Eitter, J. J. 1991, private communication
Eker, Z. 1986, MNRAS, 221, 947
Fekel, F. C., Bopp, B. W., & Lacy, C. H. 1978, AJ, 83, 1445
Fernandes, M. 1983, BAV Rundbrief, 32, 119
Hall, D. S. 1986, ApJ, 309, L83
Hall, D. S. 1990a, AJ, 100, 554
Hall, D. S. 1990b, in Active Close Binaries, edited by C. Ibanoglu (Kluwer, Dordrecht), p. 95
Hall, D. S. 1991, in The Sun and Cool Stars: Activity, Magnetism, and Dynamos, edited by I. Touminen, G. Rüdiger, and D. Moss (Springer, Berlin), p. 353
Hall, D. S. 1994, MSAIt, 65, 73
Hall, D. S., & Busby, M. R. 1989, in Remote Access Automatic Telescopes, edited by D. S. Hayes and R. M. Genet (Fairborn, Mesa), p. 187
Hall, D. S., & Busby, M. R. 1990, in Active Close Binaries, edited by C. Ibanoglu (Kluwer, Dordrecht), p. 377
Hall, D. S., Fekel, F. C., Henry, G. W., Barksdale, W. S. 1991a, AJ, 102, 1808
Hall, D. S., & Genet, R. M. 1988, Photoelectric Photometry of Variable Stars (Willmann-Bell, Richmond)
Hall, D. S., Gessner, S. E., Lines, H. C., & Lines, R. D. 1990, AJ, 100, 2017
Hall, D. S., & Henry, G. W. 1990, in Active Close Binaries, edited by C. Ibanoglu (Kluwer, Dordrecht), p. 287
Hall, D. S., & Henry, G. W. 1992a, IBVS No. 3693
Hall, D. S., & Henry, G. W. 1992b, AJ, 104, 1936
Hall, D. S., & Henry, G. W. 1993, IAU Colloquium No. 136, p. 205
Hall, D. S., & Henry, G. W. 1994, IAPPP Comm. No. 55, 51
Hall, D. S., Henry, G. W., & Sowell, J. R. 1990, AJ, 99, 396
Hall, D. S., *et al.* 1991b, JAA, 12, 281
Henry, G. W., & Hall, D. S. 1994, IAPPP Comm. No. 55, 36
Huisong, T., & Xuefu, L. 1987, A&A, 172, 74
Lucy, L. B., & Sweeney, M. A. 1971, AJ, 76, 554
Pearce, J. A. 1957, Trans. IAU, 9, 441
Scarfe, C. D., Batten, A. H., & Fletcher, J. M. 1990, PDAO, 18, 21
Strassmeier, K. G., Hall, D. S., Fekel, F. C., & Scheck, M. 1993, A&AS, 100, 173
Tassoul, J. L. 1988, ApJ, 324, L71
Tokovinin, A. 1987, Astr. Zh. 64, 196
Tout, C. A., & Hall, D. S. 1991, MNRAS, 253, 9